Electron Counts for Face-Bridged Octahedral Transition Metal Clusters

Peng-Dong Fan, Peter Deglmann, and Reinhart Ahlrichs*[a]

Abstract: Kohn–Sham orbital energy patterns were used to rationalize valence electron counts for stable face-capped octahedral clusters $[M_6E_8L_6]$ (E = S, Se, Te, Cl; L = CO, PMe_3, Cl^-). When L is a π acceptor such as CO or PMe_3, stable closed-shell clusters are found for 80, 84, and 98 electrons. For $L = Cl^-$ (i.e. a π-electron donor), only a count of 84 electrons appears favorable, as is found in $[Mo_6Cl_{14}]^{2-}$. These counting rules apply to fivefold coordination of M, which becomes unstable if the electron count exceeds 98, for example, for M = Ni. In this case structures with tetrahedrally coordinated M are energetically favored, and this leads to different cluster structures.

Keywords: cluster compounds · density functional calculations · metal–metal interactions · transition metals

Introduction

Electron-counting rules establish relationships between molecular structures and the number of valence electrons; they constitute an important concept in the chemistry of transition metal complexes and (electron-deficient) polyhedral compounds.[1, 2] Here we consider striking exceptions to these rules, namely, the clusters $[M_6E_8L_6]$, where M is a transition metal; E a face-bridging main group atom such as S, Se, or Cl; and L a two-electron donor like PR_3, CO, or Cl^-. A representative structure is shown in Figure 1. The M_6E_8 cluster core has nearly O_h symmetry, which is slightly broken by the ligands if they have lower symmetry than C_{4v}. Interest in these and related clusters comes from their rich chemistry. Chevrel phases[3] with a typical formula MMo_6E_8 (M = Li, Ca, Au, Ba,…; E = S, Se, Te) have been much investigated because of their superconducting properties. Hughbanks and Hoffmann[4] elucidated the electronic structure by extended Hückel theory (EHT) calculations on clusters such as Mo_6E_8, Mo_6E_{14}, and a variety of related solids. They point out that the 12 highest occupied levels are of primarily bonding Mo d character, consistent with a (formal) count of 24 Mo d electrons. Recent reviews by Saito,[5] Perrin,[6] and Bronger[7] describe the impressive variety of (ternary) compounds based on octahedral M_6X_{14} building blocks, which may be linked by one or more X atoms to give a typical formula $M'M_6X_{14-m}$ ($m = 0, 1, 2,\ldots$; M′ = another metal).

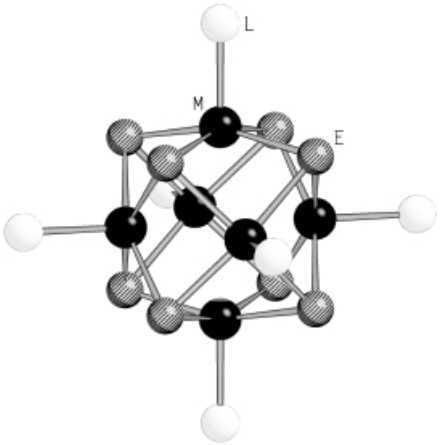

Figure 1. Structure of $[M_6E_8L_6]$, (M = Cr, Mn, Fe, Co; E = S, Se, Te, Cl; L = PMe_3, PEt_3, Cl^-).

Here we are concerned with isolated molecular clusters. Known compounds of this class[8] include transition metals Cr, Mo, W, Re, Fe, Co, Rh; face-bridging atoms S, Se, Te, Cl; and ligands PR_3, CO, Cl^-.[9–15] The valence electron count ranges from 80 to 98 if one includes the electron pairs of the metal–ligand bonds and the valence p electrons of μ_3-E. Most striking is here the considerable variation in the number of valence electrons, which is hard to reconcile with simple counting rules. In an ionic picture one could assign 48 electrons to p(E), the valence p electrons of E, and 12 electrons to the metal–ligand bonds M–L, which leaves 20 to 38 electrons for the metal cage. The listing of Lin and Williams[8] contains numerous examples with 24 electrons, some with counts of 20 and 38, and one cluster with 32 ($Fe_6S_8L_6$). Besides these there are a few cases with one electron more or less than in the above examples, which correspond to reduced or oxidized species of the parent clusters.

[a] Prof. Dr. R. Ahlrichs, Dr. P.-D. Fan, Dipl.-Chem. P. Deglmann
Theoretical Chemistry
Institute of Physical Chemistry
University of Karlsruhe
76128 Karlsruhe (Germany)

  0947-6539/02/0805-1059 $ 17.50+.50/0

If metal–metal bonding is invoked, then Wade's $14n+2$ rule would lead to the 86 electrons typical for octahedral M_6 clusters.[2] This count is apparently not found here and is shown below to exhibit a high-lying HOMO and a second-order Jahn–Teller distortion from O_h symmetry. The most abundant case, 84 electrons, that is 24 for the metal cage, would correspond to electron-pair bonds for the 12 edges of the M_6 octahedron,[1] a proposal which has not been carefully investigated or verified.

Numerous exceptions to counting rules are discussed and partly rationalized in the literature.[2] The term "rule" implies an approximate character as opposed to a law deduced from quantum mechanics. Support for the counting rules comes mainly from a wealth of experimental data. Case studies applying EHT played an important role and provided some understanding of the molecular electronic structure, especially in connection with the isolobal analogy developed by Hoffmann et al.[16] Simple (metal) orbital interaction concepts have been employed[8] to rationalize in a qualitative way the electronic structure of the clusters considered here. Rules are ideally justified within model considerations, provided a model can be defined which is sufficiently accurate and still simple enough to facilitate interpretations (e.g., tensor surface harmonic analysis).[17, 18] All these considerations are based on quite drastic simplifications and cannot be expected to provide a detailed and reliable picture of the molecular electronic structure, as will also be shown here.

We pursued a different route by treating a variety of transition metal complexes by density functional theory (DFT) methods, which give a satisfactory description of structure and energetics of the clusters of interest. However, this clear advantage is associated with the disadvantage that the electronic structure is difficult to interpret. From the results we deduce that stable closed shell cases occur only for certain electron counts which are stable with respect to changes in metal and ligands. The corresponding counting rules reflect patterns of MO diagrams which are also stable across a series of compounds and show easily rationalized trends. With this procedure we avoid the introduction of further assumptions but still obtain quite general results.

Basic Concepts and Details of Calculations

General considerations: Calculations were carried out with the RI-DFT (RI = resolution of the identity) method[19, 20] as implemented in TURBOMOLE.[21, 22] We employed the BP86 functional,[23–25] an SV(P) basis[26] (split valence plus polarization, except for H), and ECPs[27] (effective core potentials) for atoms beyond Kr. Test calculations with larger basis sets such as TZVP (triple zeta valence plus polarization),[28] resulted in virtually identical results. The computational procedure employed has the advantage of giving structural data in close agreement with experiment, as shown by the comparison in Table 1. Calculated bond lengths typically agree with experimental values to within a few picometers, which is almost within experimental errors; some exceptions will be discussed below. BP86 also gives reasonable binding energies, as was verified recently.[29–31] Hartree–Fock (HF) treatments are much less reliable in these respects and are therefore not well suited for the present purposes (see below). The PR_3 ligands were modeled by PMe_3. The clusters $[M_6E_8(PMe_3)_6]$ can then have at most D_{3d} symmetry. The M_6E_8 polyhedron is only slightly distorted from O_h, however, as is also apparent from the data in Table 1. The minor distortions permit the splitting of levels which occurs on going from O_h to D_{3d} (e.g., $t_{1u} \rightarrow a_{2u} + e_u$) to be reverted, and we can assign O_h symmetry even if the cluster has only D_{3d} symmetry. We also replaced PR_3 by CO, since this yields exact O_h symmetry. CO and PR_3 are both σ-donor and π-acceptor ligands, and we did not observe any considerable effect on the geometric or electronic structure on interchanging these ligands. For the carbonyl cases we always computed analytical second derivatives to determine whether structures correspond to a local minimum.

Table 1. Comparison of experimental and calculated bond lengths [pm] for $[M_6E_5L_6]$: DFT result/experiment.[a]

M	E	M–E	M–P	M–M	Ref. (exptl)
Co	S	224.8–225.0/223.3	212.0/213.5	276.6–278.4/282.6	[113]
Co	Se	235.5–236.1/233–237	212.6/216.2–217.5	288.9–292.3/299–302	[14]
Co	Te	253.9–255.6/250.8–254.1	213.3/213.0–216.1	310.1–319.6/323.3–327.4	[14]
Rh	S	240.8–240.9/237–239	222.3/225–226	303.3–303.8/296	[15]
Cr	S[b]	232.0–233.1/234.0–235.0	239.0/238.3	245.5–245.6/265.5–271.6	[11]
Cr	S[c]	230.2–233.3/232.7–234.2	244.4/239.5	246.0–247.8/259–260	[11]
Mo	S	249.5–250.1/243.9–244.9	254.3/252.7	269.0/266.2–266.4	[9]
W	S	252.5–253.3/243.6–247.2	254.9/251.8–252.5	273.1/267.4–268.5	[10]
Re	Se[d]	257.2–258.8/249.8–253.8	248.4–248.5/248.8–251.0	270.7–272.4/263.0–267.6	[44]

[a] Experimental data for $L = PEt_3$, calculation for $L = PMe_3$. [b] Experiment and calculation for $L = PMe_3$. [c] Experiment and calculation for $L = PEt_3$. [d] Experiment for $[Re_6Se_8I_2(\mu\text{-dpph})_2]$ (dpph = $Ph_2P(CH_2)_6PPh_2$), calculation for $[Re_6Se_8I_2(PMe_3)_4]$.

The O_h (effective) symmetry has the great advantage that only a few symmetry-adapted atomic orbitals (SAO) occur in each irreducible representation; their mixing to give MOs (molecular orbitals) can thus be discussed with confidence in a qualitative way. The reduction from AOs to SAOs is presented in Table 2, since it is needed repeatedly. In Table 2 we have only included metal nd and $(n+1)$s AOs but not the $(n+1)$p, which is discussed in the following subsection. We point to a special feature apparent from Table 2: there is only a single a_{2g} orbital, arising from metal d AOs, which is consequently M–E and M–L nonbonding. This MO is formally M–M antibonding, since there is a change in phase between all pairs of neighboring metal atoms. This matters only for sufficiently small distances when the d(M) overlap; at larger distances this MO is effectively nonbonding.

0947-6539/02/0805-1060 $ 17.50+.50/0 *Chem. Eur. J.* **2002**, *8*, No. 5

Table 2. Irreducible representations arising from atomic orbitals of octahedral clusters $[M_6E_8L_6]$

	a_{1g}	a_{2g}	e_g	t_{1g}	t_{2g}	a_{2u}	e_u	t_{1u}	t_{2u}
$s + d_{z^2}(M)$	2		2					2	
$d_\pi(M)$[a]				1	1			1	1
$d_{xy}(M)$[a]					1	1	1		
$d_{x^2-y^2}(M)$[a]		1	1						1
p(E)	1		1	1	2	1	1	2	1
σ(L)	1		1					1	
$n = 80$[b]	3	0	2	1	3	1	1	4	2
$n = 84$[b]	3	0	3	1	3	1	1	4	2
$n = 98$[b]	3	1	3	2	3	1	1	4	3

[a] The subscripts of d are given for M on the z axis; $d\pi = (d_{zx}, d_{zy})$. [b] Occupations for electron counts of 80, 84, and 98.

Some clusters considered here show metal–metal distances similar to those found in the corresponding bulk metals. This raises the question of metal–metal bonding, especially for Cr and Mo. One has to distinguish here between nd and $(n+1)$s AOs: overlap between $(n+1)$s AOs becomes effective at larger interatomic distances than that between the nd AOs. For this reason s–s bonding is more likely than d–d bonding, and the latter requires special pleading.

In subsequent discussions we will frequently refer to trends in Kohn–Sham orbital energies ε_{KS} across a series of compounds, which require some comments. The ε_{KS} of occupied MOs are always too high, that is, too close to zero. This effect is more pronounced for nd than for $(n+1)$s, which is well understood.[32] This feature is due to the (unphysical) interelectronic self-interaction included in the Coulomb term, which is incompletely canceled by the exchange term in all common functionals. Despite this deficiency, the ε_{KS} have a great advantage since they provide a reliable measure of the energy content of MOs in the sense of the aufbau principle.[33] Electrons removed or added to reach ionic ground states always involve the HOMO or LUMO; exceptions to this rule only occur if there are virtually degenerate levels. Differences in ε_{KS} are furthermore a good approximation to electronic excitation energies.[34] All these features imply that a low-lying HOMO and a high-lying LUMO indicate chemical stability, for example, in the sense of frontier orbital considerations.

This is a great advantage over HF treatments, which always stabilize occupied and destabilize unoccupied MOs, and hence typically yield a HOMO–LUMO gap that is too large. If HOMO and LUMO have different symmetry, one usually obtains $\varepsilon_{HOMO} < \varepsilon_{LUMO}$, even if the occupation is incorrect. Therefore, a converged HF calculation usually gives no indication of whether the chosen occupation is appropriate, that is, leads to the lowest total energy. The only certain way to find the best occupation in the sense of the variation principle is to perform HF calculations for all occupations which appear reasonable. For this reason HF treatments are of little help in establishing directly the energetic ordering of MOs in the sense of the aufbau principle, and they are not well suited for the present purpose.

To conclude this section we mention some (minor) details of calculations. All structure optimizations were carried out within the restricted Kohn–Sham (RKS) method for closed-shell states and with UKS (unrestricted KS) for open shells in the high-spin states. The arrows representing electron spin in the figures presented below thus give a complete description of the character of the total wavefunction. The UKS procedure leads to a splitting of α and β MO levels. To simplify MO diagrams we have neglected spin polarization in the figures, which basically implies an averaging of α and β orbital energies for doubly occupied MOs. The total charge of a molecular cluster has a strong influence on the orbital energies, which are considerably shifted upwards for anions without changing the order of ε_{KS}. For a better comparison of MO diagrams of a sequence of compounds, we have thus reduced the occupation of the HOMO in anions such that the systems compared are effectively neutral.

On the importance of $(n+1)$p transition metal orbitals: The importance of $(n+1)$p AOs for a description of bonding in transition metal complexes is still controversial, as is demonstrated by two recent articles. Landis, Firman, Root, and Cleveland (LFRC)[35] summarized reasons and evidence for the relative unimportance of $(n+1)$p orbitals; Bayse and Hall (BH)[36] stressed their role particularly for larger (formal) d occupations. There is agreement that nd and $(n+1)$s are more important than $(n+1)$p, and that the latter matter especially for covalent bonding. The two articles[35, 36] discuss mainly transition metal hydrides. Since the controversy has a bearing on the present considerations we briefly comment on this problem.

LFRC point out that many transition metal compounds must be considered as hypervalent if $(n+1)$p orbitals are not involved in bonding. BH find this view difficult to accept. They consider ClH_3 and $[PdH_3]^-$ in the T-shaped equilibrium structures for a detailed comparison to demonstrate their point. ClH_3 was chosen as a simple model case for a typical hypervalent compound with a three-center, four-electron bond, which can be decribed as a resonance [Eq. (1)]. This

$$H_{eq}^- \; Cl{-}H_{eq} \leftrightarrow H_{eq}{-}Cl \; H_{eq}^- \qquad (1)$$

description is confirmed by a population analysis which indicates "that only 1.7 % of chlorine electrons are located in d orbitals" and the fact that localization of occupied MOs was not possible. However, it was also pointed out that d contributions (at Cl) "stabilize the molecule by 37.8 kcal mol^{-1}" (158 kJ mol^{-1}) at the RHF level. BH employed a triple-ζ basis for hydrogen, which is reasonable since hydrogen carries a negative charge. Including the p polarization functions (at H) in this comparison reduces the stabilization by d at Cl to 125 kJ mol^{-1}. We employed a TZVP basis[28] for H in the RHF calculations on hydrides discussed in this subsection.

A different picture is presented for $[PdH_3]^-$, again at the RHF level. An analysis of the wavefunctions shows three localized MOs which describe Pd–H bonds, "and that the Pd–H_{eq} bonds have almost a 1:1:1 ratio for s, p, and d character" at Pd. This is considered to be consistent with the fact that "there are no 4d orbitals of proper symmetry to form a T-shaped structure" for $[PdH_3]^-$. The case appears to be clear cut: $[PdH_3]^-$ must be described by spd^5 hybridization

and it is not a hypervalent compound (unlike ClH_3). BH did not report the energetic stabilization due to the 5p orbitals, which amounts to a mere 26 kJ mol^{-1}. The Pd 5p function also has only a small influence on the molecular geometry; the bond lengths are affected by only 1.5 pm, and the H_{ax}-Pd-H_{eq} angle remains at 89°. BH further consider $[RhH_4]^-$ (in the sawhorse C_{2v} structure) and $[WH_7]^-$ (in the capped trigonal antiprismatic structure) as problem cases for a hypervalent description. The effect of $(n+1)$p on structure and energy is here the same as described for $[PdH_3]^-$; the 6p at W lowers the energy by only 16 kJ mol^{-1}.

We next consider $[Ni(CO)_4]$ as a textbook example for the 18-electron rule, which assumes that Ni 4p orbitals are involved in bonding. Excluding the 4p basis set on Ni affects the Ni–C distance by less than 1 pm, and the binding energy ($[Ni(CO)_4] \rightarrow Ni(^3F) + 4\,CO$) by 66 kJ mol^{-1}, roughly 15% of the total binding energy, which indicates a relatively small effect of 4p functions. A similar state of affairs is found for the clusters considered here. For $[Cr_6S_8(CO)_6]$ we obtain a stabilization of 35 kJ mol^{-1} per Cr atom resulting from the 4p orbital of Cr. The bond lengths are affected by at most 1.7 pm. We note that the energetic stabilization effected by an orbital is a useful measure for its importance in bonding.[37] Different conclusions were drawn for $[W(CO)_6]$ and the isoelectronic series in which W is replaced by Hf^{2-} to Ir^{3+}.[38] An energy analysis indicates the metal 6s and 6p to be of roughly equal importance. Calculations with and without the 6p set lead to only minor changes in the energy, and there may be a problem in the analysis which deserves further consideration.

The above examples provide an estimation of the importance of $(n+1)$p metal orbitals for cases in which they are usually considered to be necessary. Our results show a virtually negligible effect of $(n+1)$p on structures (1–2 pm) and a moderate energetic stabilization which is smaller than that typically found for polarization functions. It thus appears reasonable to consider only *n*d and $(n+1)$s for a discussion of gross features of the molecular electronic structure of the clusters considered here. All calculations on the octahedral clusters were, of course, carried out with $(n+1)$p functions included in the basis set.

Counting Rules

Low-lying orbitals: We base our analysis of clusters $[M_6E_8L_6]$ on a comparison of compounds with increasing atomic number of M and accordingly increasing number of electrons. The electrons of interest for the present purpose include the σ electron pairs of the ligands σ(L) (involved in M–L bonding), the valence p electrons p(E), and the valence electrons of M. Figure 2 shows a diagram of orbital energy levels for a series of clusters with different metals and L = CO as model ligand. This facilitates the discussion, since the occupied ligand MOs are lower in energy than the cluster MOs of interest here.

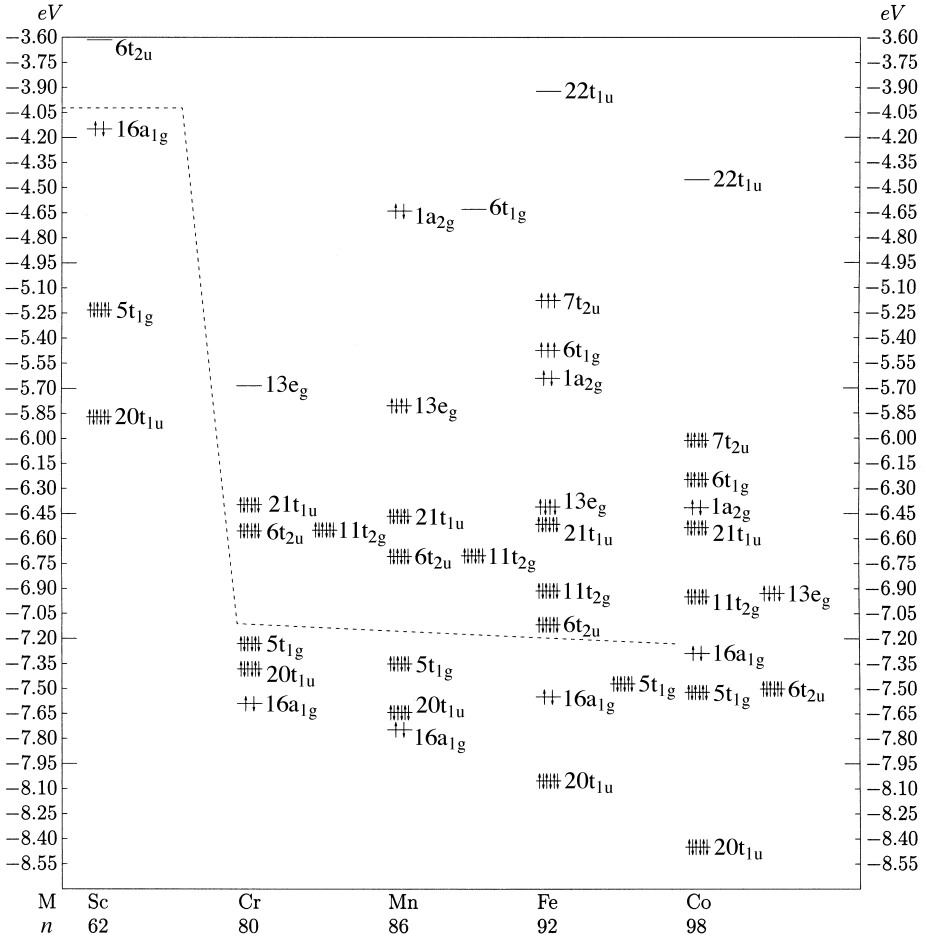

Figure 2. The energy of molecular obitals of $[M_6S_8(CO)_6]$; the levels below the dashed line are low-lying states according rule a. *n* denotes the number of cluster valence electrons, as described in the text.

Rule a: The lowest lying valence cluster MOs correspond to the irreducible representations arising from σ(L) and p(E) and one additional a_{1g} MO for a total of 62 electrons.

The number and symmetries of these MOs are: 3^*a_{1g}, 2^*e_g, t_{1g}, 2^*t_{2g}, a_{2u}, e_u, 3^*t_{1u}, and t_{2u}. According to Table 2 all MOs from σ(L) and p(E) have sufficient counterparts from metal s and d with which they can interact, and the resulting MOs are bonding (or slightly antibonding at worst). The additional a_{1g} arises mainly from metal s, with some d_{z^2} contributions, and corresponds to the bonding radial σ MO familiar from the rules of Wade or Wade and Mingos.[1, 2]

  0947-6539/02/0805-1062 $ 17.50+.50/0 *Chem. Eur. J.* **2002**, *8*, No. 5

In the limit of ionic bonding there are 60 electrons from σ(L) and p(E). This case is almost realized by $[Sc_6S_8(CO)_6]$ with 62 electrons. The additional a_{1g} is the HOMO (see Figure 2), but this is embedded within the other MOs in the remaining cases. The occupied valence MOs of the M_6E_8 core are predominantly located on E for M = Sc (with the exception of the highest a_{1g}); with increasing atomic number and the ensuing stabilization of metal d, these MOs will clearly receive increasing d contributions and may even be predominantly of metal d character.

The O_h structure of neutral $[Sc_6S_8(CO)_6]$is a saddle point on the potential surface, whereas the dication is a local minimum. This result is in line with the spacing of high-lying MOs, since the dication has a larger HOMO–LUMO gap than the neutral cluster. The dication $[Sc_6S_8(CO)_6]^{2+}$ can of course be considered as a cluster with normal oxidation states Sc^{3+} and S^{2-}.

π-Acceptor ligands: Since the first group of MOs is M–E and M–L bonding, the next MOs to be occupied should be nonbonding or slightly antibonding. This condition is met for those d(M) which interact only relatively weakly with p(E) or σ(L) orbitals, since bonding and antibonding of the resulting MOs is then also weak. Clearly, d_{z^2}(M) and d_{xy}(M) should be excluded for this purpose, since these d functions have largest overlap with σ(L) and p(E) orbitals, respectively, as sketched in Figure 3 for p(E).

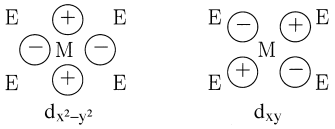

Figure 3. Sketch of metal d_δ orbitals in a local coordinate system.

The situation is different for $d_{x^2-y^2}$(M), which give rise to a_{2g}, e_g,and t_{2u} SAOs (Table 2). The maxima of $d_{x^2-y^2}$ are located between E atoms, and overlap with p(E) is thus minimized (Figure 3). The a_{2g} orbital has no counterpart with which it can interact and is of pure d character. Matters are similar for d_π(M), which yield t_{1g}, t_{2g}, t_{1u}, and t_{2u}. These orbitals are stabilized by π backbonding, a slight delocalization into π*(L). Besides lowering the energy this also reduces overlap with p(E), which is not very pronounced anyway. Since M and the four neighboring E are almost in the same plane (Figure 1), a $d_\pi - p_\pi$ situation arises in which overlap is much smaller than for d_{xy}–p(E), as noted above.

From the DFT calculations we obtain the following energetic ordering of the MOs: $6t_{2u} \approx 11t_{2g} \approx 21t_{1u} \leq 13e_g \leq 1a_{2g} \approx 6t_{1g} \approx 7t_{2u}$.

The first group of MOs ($6t_{2u}$, $11t_{2g}$, $21t_{1u}$) is virtually degenerate. The compounds with M = Ti, V are expected to be relatively unstable open-shell systems, which furthermore show Jahn–Teller distortions from O_h symmetry. This group of MOs is fully occupied for M = Cr with 80 electrons. The O_h structure is a local minimum, in agreement with the fact that the LUMO $13e_g$ is well separated from the HOMO. The $13e_g$ MO in turn is separated by a considerable gap from the next higher MOs. In agreement with this pattern we find $[Mn_6S_8(CO)_6]^{2+}$ with 84 electrons to be a local minimum with O_h structure, whereas the neutral closed-shell cluster is a saddle point on the potential surface, that is, we find a second-order Jahn–Teller distortion. Furthermore, the near degeneracy of $1a_{2g}$ and $6t_{1g}$ leads to several triplet states (energetically lower than the closed-shell case), and reults in first-order Jahn–Teller distortions to D_{3d} and D_{4h} molecular symmetry.

For Fe and Co we find the MOs $1a_{2g}$, $6t_{1g}$, $7t_{2u}$ to be close in energy, and these MOs are fully occupied for M = Co with a considerable HOMO–LUMO gap that leads to an O_h minimum. Due to the near degeneracy of $1a_{2g}$, $6t_{1g}$, and $7t_{2u}$, one expects high-spin states for a partial occupation according to Hund's rules. For $[Fe_6S_8(CO)_6]^+$ only seven electrons occupy the MOs with parallel spins ($S = 7/2$). For the neutral cluster the $1a_{2g}$ MO is doubly occupied, and $6t_{1g}$ and $7t_{2u}$ are half-filled with $S = 3$. These results agree with experiment for the corresponding clusters with $L = PR_3$.[12, 39]

The above discussion is summarized in a rule which complements rule a.

Rule b: If L is a π acceptor, up to 36 additional electrons can occupy MOs which are roughly nonbonding; stable closed-shell cases also occur for 18 and 22 electrons, resulting in total electron counts of 80, 84, and 98.

Note that the pattern of orbital energies is remarkably stable across the series of compounds depicted in Figure 2. The only slight change concerns $16a_{1g}$, which is located above the lowest MO (rule b), $6t_{2u}$, for M = Co.

Since we try to avoid the introduction of model considerations as much as possible, we point only to a few features obvious from Figure 2. It is possible to discern different types of MOs. Those that remain roughly constant in energy from Cr to Co describe MOs of dominant ligand character; a good example is $21t_{1u}$. This behavior contrasts with that of the MOs $1a_{2g}$, $6t_{1g}$, and $7t_{2u}$ (and other low-lying orbitals), which are considerably stabilized with increasing atomic number of M. This group includes $1a_{2g}$, the only pure d MO; one can thus assign these orbitals a dominant metal d character. For some other MOs a corresponding change in ε_{KS} occurs between Sc and Cr (e.g., $6t_{2u}$, $11t_{2g}$, $13e_g$, $21t_{1u}$).

The 98-electron case (M = Co) can be viewed from a different angle. The 36 electrons from rule b were assigned exclusively to symmetries to which d_π and $d_{x^2-y^2}$ contribute. The corresponding irreducible representations are thus quite crowded, with a_{2g}, t_{1g}, and t_{2u} fully occupied (see Table 2). This suggests describing the metal atom approximately as a d^6 case, with d_π and $d_{x^2-y^2}$ almost fully occupied. Bonding to E and L is then effected by d_{z^2}, d_{xy}, and s contributions to delocalized cluster MOs. This reasoning is compatible with the formal oxidation state of Co ($q = 2⅔$), which implies a d-occupation around d^7.

π-Donor ligands: The above reasoning requires some modifications if the ligand L is a π donor, as in $[Mo_6Cl_{14}]^{2-}$. The p_π electrons of L are now embedded within the cluster MOs of rule a; their interaction with metal d_π MOs leads to changes in MO diagrams which are difficult to follow or rationalize in detail. We thus rely on DFT calculations, which yield the MO diagram presented in Figure 4 for M = Nb, Mo, Tc. This shows

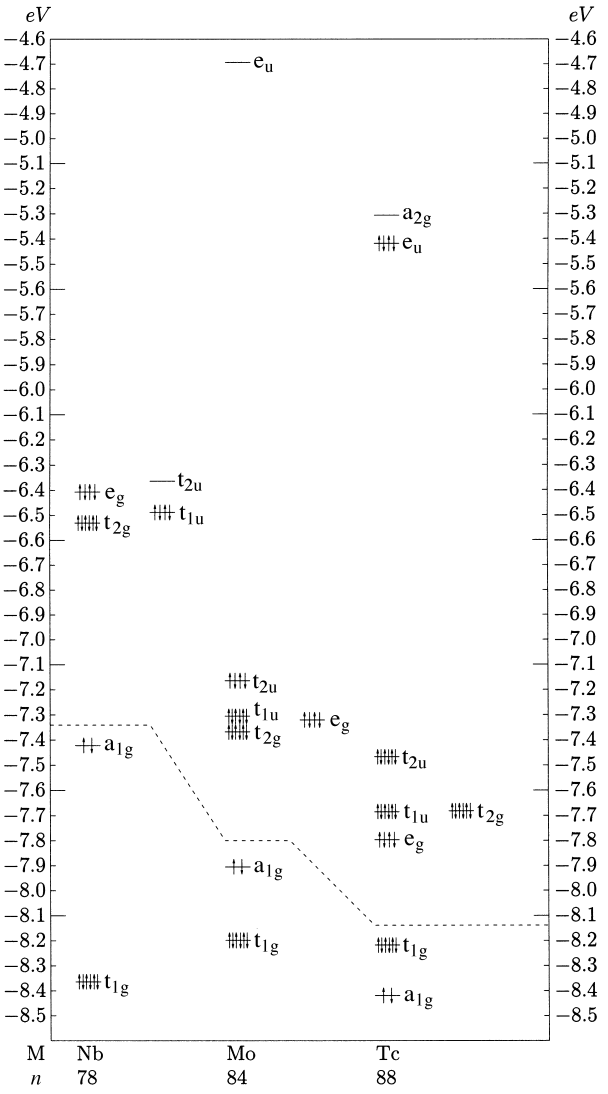

Figure 4. The energy of molecular orbitals of $[Nb_6Cl_8Cl_6]^{2-}$, $[Mo_6Cl_8Cl_6]^{2-}$, and $[Tc_6Cl_8Cl_6]$. The levels below the dashed line are low-lying states according to rule a. For better comparison all systems were calculated in neutral state by lowering the occupation of the HOMO, as explained in the text. The complete assignment of MOs is: $l3a_{lg}$, $5t_{lg}$, $10e_g$, $18t_{1u}$, llt_{2g}, $6t_{2u}$, $3e_u$, and la_{2g}, when an ECP(28) is employed for the transition metal.

first of all that the 62-electron line of rule a holds here as well. For the remaining MOs one has:

Rule b′: If L is a π donor up to 22 electrons can occupy MOs which are of essentially nonbonding d(M) type, resulting in a total count of 84.

The dominant feature of Figure 4 is the pronounced HOMO–LUMO gap for the 84-electron case. Since a large gap is a simple and reliable indicator of stability with respect to chemical reactions or geometry distortions, Figure 4 expresses a preference of isolated clusters of this type for 84 electrons for which there are few exceptions (see below). An increase in the the number of electrons requires the occupation of high-lying MOs (e.g., for M = Tc) from which they are more easily removed by oxidation than for M = Mo. The closed-shell case indicated in Figure 4 is less stable than open-shell triplet states which cause first-order Jahn–Teller distortions to D_{4h}. With fewer than 84 electrons (e.g., M = Nb) one finds a typical multireference situation, since the orbitals e_g, t_{2g}, t_{1u}, and t_{2u} in Figure 4 are almost identical in energy.

The MO diagram shown in Figure 4 is remarkably robust with respect to changes in M and the replacement of Cl by other atoms. $[Cr_6Cl_{14}]^{2-}$ shows the very same features as the corresponding Mo cluster. A related cluster is $[Re_6Se_8I_6]^{4-}$, which also has 84 cluster electrons. Electronic structure calculations for systems of this (small) size and (high) charge are not reasonable, in agreement with the fact that they are unstable in the gas phase and eject electrons. This may explain the fact that only $[Re_6Se_8I_6]^{3-}$ with 83 electrons is known. Calculations with reduced occupation of the HOMO, to account approximately for the effect of counterions, show the same picture as Figure 4. Another exception to rule b′ is $Na[W_6Br_{14}]$[40] with 83 electrons for $[W_6Br_{14}]^-$. These examples show that it is possible to oxidize clusters with 84 electrons, which leads to clusters weakly distorted from O_h symmetry.

A rather extreme example for studying the stability of the MO pattern is $[Re_6(\mu_3\text{-}S)_4(\mu_3\text{-}Cl)_4Cl_6]$, which has also 84 electrons. In this cluster[41] the μ_3 positions are occupied statistically by S and Cl. We have considered the T_d ("heterocubane") and the C_{4v} ("all-*cis*") structures; the latter is calculated to be 138 kJ mol^{-1} lower in energy. Both structures are local minima on the potential surface. The MO diagrams show a pronounced HOMO–LUMO gap with virtually degenerate levels at the HOMO energy, as in Figure 4.

The only common feature of the diagrams presented in Figures 2 and 4 concerns the low-lying metal-cage MOs, which are of symmetry e_g, t_{2g}, t_{1u}, t_{2u} in both cases. These MOs are now very close in energy (Figure 4), and cases with 80 electrons will normally not be stable; this is a pronounced difference to Figure 2. Another difference concerns the MOs of higher energy than this group, which have different symmetries: the e_u MO of Figure 4 is very high lying in Figure 2. These are essential details which are not reflected by the qualitative considerations of Lin and Williams[8]: the cases b and b′ are markedly different.

Chevrel phases also exhibit electron counts lower than 84, typically down to 80. Perrin pointed out that the corresponding clusters are not discrete in these cases and that "the connection between the units introduces additional features".[6] We could not carry out band structure calculations to investigate this problem, but we can offer the following rationalization. The 80-electron case in Figure 4 does not lead to a pronounced HOMO–LUMO gap. Replacing the π donor L by a π acceptor stabilizes of the levels t_{2g}, t_{1u}, and t_{2u} arising from d_π(M) (see Table 2), which leads to a sufficiently large HOMO–LUMO gap for the 80-electron case to be stable (Figure 2). A transition between the two situations requires the possibility to tune the π-acceptor/donor properties of L. Exactly this is expected to happen if Cl^- ions, for example, act as a link between two units, which should reduce their π-donor capability.

Metal–metal bonding: The low-lying metal cage MOs considered in rules b and b′ belong to symmetries e_g, t_{2g}, t_{1u}, and t_{2u}. These are precisely the bonding SAOs resulting from metal d_π and $d_{x^2-y^2}$ AOs,[8] and this raises the question of

0947-6539/02/0805-1064 $ 17.50+.50/0 *Chem. Eur. J.* **2002**, *8*, No. 5

metal–metal bonding. We tackle this problem in a simple way and consider trends in intermetallic distances in the series $[M_6E_8(CO)_6]$ (M = Cr, Co; E = S, Se, Te). The calculated M–M distances are Cr–Cr: 247 (E = S), 252 (Se), 260 (Te); Co–Co: 279 (S), 290 (Se), 306 pm (Te).

The Co–Co distances are significantly larger than the value in the bulk metal (250 pm), and there is no reason to discuss intermetallic bonding. This view is confirmed by the respective increases in Co–Co distance by 11 and 27 pm on going from S to Se and Te, which reflects the increasing radius of E. For the complexes of Cr, the bond lengths are in the range of those in the bulk metal (258 pm). Even more important is the only moderate increase in the Cr–Cr distance by only 5 and 13 pm from S to Se and Te, respectively. The Cr_6 octahedron is much more resistant to an extension enforced by the increasing size of E than Co_6. If bond lengths are accepted as an indicator of bonding, the trends displayed by DFT results clearly point to some intermetallic bonding in the complexes of Cr but not in those of Co. We cannot estimate the contribution of Cr–Cr interactions to the binding energy or force constants, but results presented below indicate that it is weak.

Complexes with L = PR_3

We next turn to L = PMe_3 as a ligand representative for PR_3 in complexes listed in Table 1. The replacement of CO by PMe_3 leads to some minor changes, since MOs of the ligands involved in P–R bonding are now embedded within the cluster MOs of group a; this is obvious and has no consequences since these MOs do not overlap with metal orbitals.

Figure 5 presents orbital energies of higher-lying MOs of $[M_6S_8(PMe_3)_6]$ (M = Cr, Mn, Fe, Co). The similarity with Figure 2 for L = CO is striking. With M = Cr, for example, a group of occupied t_{2g}, t_{1u}, and t_{2u} MOs lies above the 62-electron line in either case, and these MOs are well separated from the other occupied or unoccupied MOs. A slight change is found in the position of the highest a_{1g} MO within group a. This orbital is at higher energy for L = PMe_3 than for CO, an effect easily rationalized by destabilizing interactions with σ(L), which are larger for PMe_3, since σ(L) is higher in energy than in CO.

We next consider replacement of Cr by Mo or W and that of Co by Rh or Ir. The corresponding MO diagrams are not shown since they show the same general picture as is displayed in Figures 2 and 5. The only change concerns a slight reordering of lower-lying levels for Rh and Ir as compared to Co.

We return to the discussion of calculated and experimental bond lengths in Table 1. Deviations of up to about 8 pm are within the (combined) error margins of experiment and DFT calculations; the latter is estimated to be about ±5 pm for the present cases. We do not dare to estimate errors arising from X-ray scattering, but an uncertainty of a few picometers is likely. Deviations larger than 8 pm occur only for M – M distances of $[Co_6Te_8(PR_3)_6]$ (ca. 10 pm) and $[Cr_6S_8(PR_3)_6]$. The experimental Cr–Cr distances are in the range of those of the bulk metal (258 pm) and change in going from L = PMe_3 to L = PEt_3. This is not reflected in the calculated distances, but we found that the calculated structure constants vary with the conformation of L = PEt_3, and it took some effort to find the low-energy structure. All we can say with some confidence is that M–M distances in this case are very sensitive to small changes in the ligand structure. This implies that these M–M bonds are relatively weak.

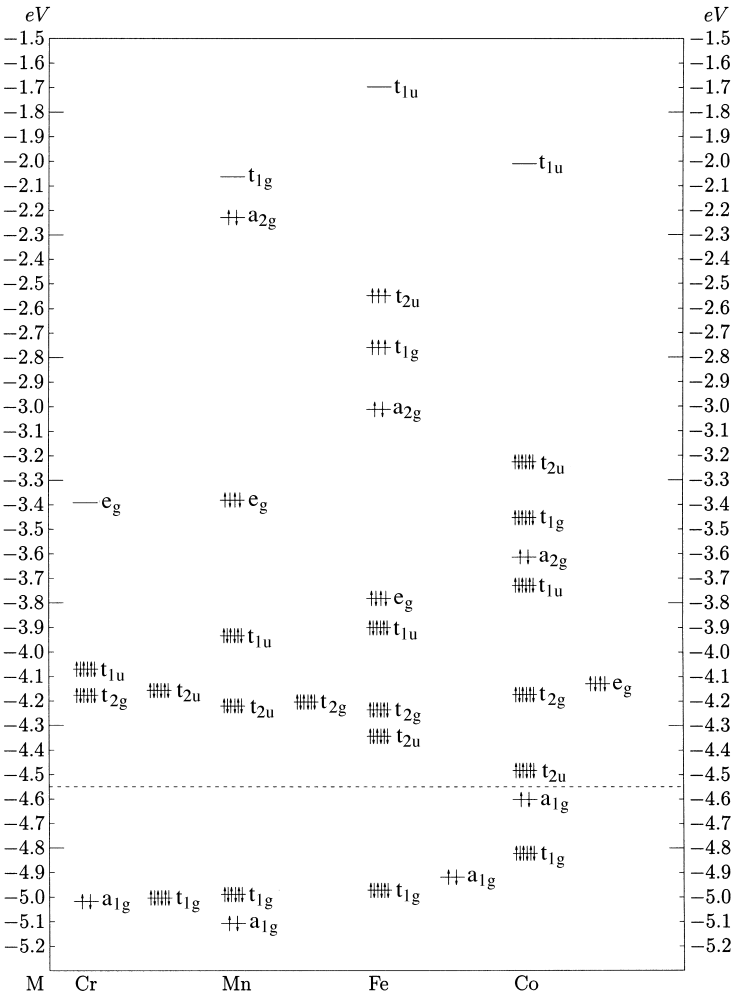

Figure 5. The energy of molecular orbitals of $[M_6S_8(PMe_3)_6]$, labeled according to irreducible representations of O_h; levels below the dashed line are low-lying states according to rule a.

We learnt of the existence of $[Rh_6S_8(PR_3)_6]$ (included in Table 1) in discussions[42] after the present calculations indicated that it is relatively stable. The compound has a total composition $[Rh_6S_8(PEt_3)_6][Rh_3Cl_6S_2(PEt_3)_3]_2$. Since the second part appears unquestionably to be an anion that is quite stable according to calculations, the octahedral cluster was tentatively assigned a charge of +2. However, the presence of undetected protons that would change the charge assignment cannot be excluded. Our calculations give relatively similar structure constants for neutral $[Rh_6S_8(PMe_3)_6]$ and its dication, and the available data do not favor one or the other possibility.

Complexes of Nickel

We have so far considered the stability of clusters shown in Figure 1 for an electron count up to 98, corresponding to M = Co. We consider $[Ni_6S_8(CO)_6]$ as a model compound for the hypothetical $[Ni_6E_8L_6]$. The electron count increases to 104, and one must occupy the high-lying MO $22t_{1u}$ in Figure 2. This MO is Ni–S and Ni–C antibonding, as can be inferred by comparing calculated bond lengths with those of $[Ni_6S_5(CO)_6]$: (Ni–S 226 versus 217 pm, Ni–C 186 vs 178 pm). This clearly indicates the octahedral complex to be unstable. Furthermore, the MO $22t_{1u}$ is nearly degenerate with $14e_g$ (not shown in Figure 2). Consequently, we find an open-shell state with $S = 2$, which leads to a first-order Jahn–Teller distortion to a D_{4h} state that is more stable than the closed-shell case. For this D_{4h} state two Ni–C distances are elongated to 191 pm, which means that these CO ligands are very weakly bound to Ni.

To rationalize this finding we return to the discussion of rule b: $[Co_6S_8(PR_3)_6]$ can be regarded as having a $3d^6$ electron configuration for Co in which two d orbitals are available for bonding to neighboring atoms, which results in a total occupation of about d^7. With the replacement of Co by Ni, the d occupation is increased to roughly d^8 (the formal occupation would be $d^{7.3}$, which represents a lower limit). Consequently, the d orbitals are now less available for bonding to E and/or L. The square-pyramidal fivefold metal coordination that is typical of the octahedral structure (Figure 1) cannot accommodate such a high d occupation and becomes unstable.

Nickel can even bind ligands in a d^{10} configuration, for example, in $[Ni(CO)_4]$, which has a tetrahedral arrangement of ligands that leads to much smaller metal–ligand interactions than in the "octahedral" fivefold coordination considered above. In the known compound $[Ni_6Se_5(PR_3)_6]$[43] Ni indeed has an approximately tetrahedral coordination environment. The metal atoms form a trigonal prism in which all faces are capped by Se, and PR_3 is attached to Ni. These facts can be expressed as a rule:

Rule c: The octahedral structure of $[M_6E_8L_6]$ with fivefold square-pyramidal coordination of M becomes unstable if the electron count exceeds 98. For M = Ni, which would lead to 104 electrons, structures with tetrahedral coordination and different cluster composition are favored.

The MO diagram of $[Ni_6Se_5(PR_3)_6]$ is not easily discussed, mainly because of the lower symmetry (D_{3h} instead of O_h). Rule a holds in this case with appropriate modifications: the lowest lying MOs (in the valence region) have the same symmetries as σ(L) and p(E), followed by an a_1' MO. The higher lying MOs are relatively densely spaced and difficult to interpret.

Conclusion

We have carried out DFT calculations on octahedral clusters $[M_6E_8L_6]$ (Figure 1) for a series of transition metals M. The essential results can be summarized as follows. If L is a π acceptor, electron counts of 80, 84, and 98 lead to closed-shell states with pronounced HOMO–LUMO gaps and a potential minimum in (approximately) O_h symmetry, whereas for 92 electrons (e.g., $[Fe_6S_8(PR_3)_6]$), a high-spin state with $S = 3$ results (Figure 2). A special case is $[Sc_6E_8L_6]^{2+}$ with 60 electrons, which is basically ionic with a d^0 occupation for Sc. If L is a π donor, only a count of 84 electrons leads to a stable closed-shell state for isolated clusters.

The stability of the O_h structure is mainly due to bonding M–E interactions; the occupation of MOs with considerable contributions from valence orbitals of E is the only common feature of stable clusters (rule a). Direct bonding between metal d orbitals plays some role for M = Cr (and Mo or W), but certainly not for M = Fe or Co and their heavier analogues, since the metal–metal distances are too large. It can also be excluded for M = Sc, which has a formal d^0 occupation.

The octahedral cluster structure becomes unstable if the electron count exceeds 98 (e.g., for M = Ni). Structures with a tetrahedral coordination of M are then energetically favored because of the large metal d occupation.

The summary as well as the considerations presented in this article are based 1) on the reliability of DFT in describing transition metal clusters and 2) the fact that the Kohn–Sham orbital energies comply with the aufbau principle. Our conclusions were essentially justified by the remarkable stability of results with respect to changes in transition metals and ligands.

The present study provides a detailed interpretation of experimental data, which was previously not available. The EHT studies[8] described some details correctly, for example, the symmetries of low-lying metal-cage MOs e_g, t_{2g}, t_{1u}, and t_{2u}, but failed in other details. They appear to miss in particular the distinction between π donor and acceptor ligands L.

Acknowledgements

We are very much indebted to Udo Radius for numerous valuable discussions and to Dieter Fenske for making unpublished results available. This work was supported by the DFG within the SFB 195 ("Lokalisierung von Elektronen in makroskopischen und mikroskopischen Systemen") and by the Fonds der Chemischen Industrie.

[1] K. Wade, "Some Bonding Considerations" in *Transition Metal Clusters* (Ed.: B. F. G. Johnson), Chap. 3, Wiley, Chichester, **1980**.
[2] D. Michael, P. Mingos, A. S. May, "Structure and Bonding Aspects of Metal Cluster Chemistry" in *The Chemistry of Metal Cluster Complexes* (Eds.: D. F. Shriver, H. D. Kaesz, R. D. Adams), Chap. 2, VCH, New York, **1990**, pp. 81–114.
[3] R. Chevrel, M. Sergent, J. Prigent, *J. Solid State Chem.* **1971**, *3*, 515
[4] T. Hughbanks, R. Hoffmann, *J. Am. Chem. Soc.* **1983**, *105*, 1150 .
[5] T. Saito, "Chalcogenide Cluster Complexes of the Early Transition Metals", in *Early Transition Metal Clusters with π-Donor Ligands* (Ed.: M. H. Chisholm), Chap. 3, VCH, New York, **1995**.
[6] C. Perrin, "M_6L_{14} and M_6L_{18} Units in Early Transition Element Cluster Compounds" in *Metal Clusters in Chemistry* (Eds.: P. Braunstein, L. A. Oro, P. R. Raithby), Chap. 5.5, Wiley-VCH, Weinheim, **1999**.
[7] W. Bronger, "Ternary Rhenium and Technetium Chalcogenides Containing Re_6 or Tc_6 Clusters" in *Metal Clusters in Chemistry* (Eds.: P. Braunstein, L. A. Oro, P. R. Raithby), Chap. 5.6, Wiley-VCH, Weinheim, **1999**.

  0947-6539/02/0805-1066 $ 17.50+.50/0 *Chem. Eur. J.* **2002**, *8*, No. 5

[8] Z. Y. Lin, I. D. Williams, *Polyhedron* **1996**, *15*, 3277.
[9] T. Saito, N. Yamamoto, T. Nagase, T. Tsuboi, K. Kobayashi, T. Yamagata, H. Imoto, K. Unoura, *Inorg. Chem.* **1990**, *29*, 764.
[10] T. Saito, A. Yoshikawa, T. Yamagata, H. Imoto, K. Unoura, *Inorg. Chem.* **1989**, *28*, 3588.
[11] K. Tsuge, H. Imoto, T. Saito, *Bull. Chem. Soc. Jpn.* **1996**, *69*, 627.
[12] C. A. Goddard, J. R. Long, R. H. Holm, *Inorg. Chem.* **1996**, *35*, 4347.
[13] F. Cecconi, C. A. Ghilardi, S. Midollini, *Inorg. Chim. Acta* **1981**, *64*, L47; F. Cecconi, C. A. Ghilardi, S. Midollini, *Inorg. Chim. Acta* **1983**, *76*, L183.
[14] S. Balter, "Synthese und Struktur tellurverbrückter Eisen-, Cobalt- und Kupfercluster", Dissertation, Universität Karlsruhe (TH), **1994**.
[15] B. O. Kneisel, "I Synthesen und Kristallstrukturen chalkogenverbrückter Clusterkomplexe der leichten Platinelemente. II Nanostrukturierte Supramolekularaggregate—röntgenstrukturanalytische Untersuchungen an Makromolekülen bei atomarer Auflösung", Dissertation, Universität Karlsruhe (TH), **1997**.
[16] R. Hoffmann, *Angew. Chem.* **1982**, *94*, 725; *Angew. Chem. Int. Ed. Engl.* **1982**, *21*, 711.
[17] R. L. Johnston, D. M. P. Mingos, *J. Organometal. Chem.* **1985**, *280*, 407.
[18] R. L. Johnston, D. M. P. Mingos, *J. Organometal. Chem.* **1985**, *280*, 419.
[19] K. Eichkorn, O. Treutler, H. Ohm, M. Häser, R. Ahlrichs, *Chem. Phys. Lett.* **1995**, *242*, 652.
[20] K. Eichkorn, F. Weigend, O. Treutler, R. Ahlrichs, *Theor. Chem. Acc.* **1997**, *97*, 119.
[21] R. Ahlrichs, M. Bär, M. Häser, H. Horn, C. Kölmel, *Chem. Phys. Lett.* **1989**, *162*, 165 (current version: http://www.chemie.unikarlsruhe.de/PC/TheoChem).
[22] O. Treutler, R. Ahlrichs, *J. Chem. Phys.* **1995**, *102*, 346.
[23] J. P. Perdew, *Phys. Rev. B* **1986**, *33*, 8822.
[24] A. D. Becke, *Phys. Rev. A* **1988**, *38*, 3098.
[25] S. H. Vosko, L. Wilk, M. Nusair, *Can. J. Phys.* **1980**, *58*, 1200.
[26] A. Schäfer, H. Horn, R. Ahlrichs, *J. Chem. Phys.* **1992**, *97*, 2571.
[27] D. Andrae, U. Haeussermann, M. Dolg, H. Stoll, H. Preuss, *Theor. Chim. Acta* **1990**, *77*, 123.
[28] A. Schäfer, C. Huber, R. Ahlrichs, *J. Chem. Phys.* **1994**, *100*, 5829.
[29] R. Ahlrichs, F. Furche, S. Grimme, *Chem. Phys. Lett.* **2000**, *325*, 317.
[30] A. Mateev, M. Staufer, M. Mayer, N. Rösch, *Int. J. Quantum Chem.* **1999**, *75*, 863.
[31] C. Adamo, M. Ernzerhof, G. E. Scuseria, *J. Chem. Phys.* **2000**, *112*, 2643.
[32] J. P. Perdew, A. Zunger, *Phys. Rev. B* **1981**, *23*, 5048.
[33] R. Bauernschmitt, R. Ahlrichs, *J. Chem. Phys.* **1996**, *104*, 9047.
[34] R. Bauernschmitt, R. Ahlrichs, *Chem. Phys. Lett.* **1996**, *256*, 454.
[35] C. R. Landis, T. K. Firman, D. M. Root, T. Cleveland, *J. Am. Chem. Soc.* **1998**, *120*, 1842.
[36] C. A. Bayse, M. B. Hall, *J. Am. Chem. Soc.* **1999**, *121*, 1348.
[37] H. Horn, R. Ahlrichs, *J. Am. Chem. Soc.* **1990**, *112*, 2121.
[38] D. Axel, F. M. Bickelhaupt, G. Frenking, *J. Am. Chem. Soc.* **2000**, *122*, 6449.
[39] A. Bencini, G. A. Ghilardi, S. Midollini, A. Orlandini, U. Russo, M. G. Uytterhoeven, C. Zanchini, *J. Chem. Soc. Dalton Trans.* **1995**, 963.
[40] Y. Q. Zheng, Y. Grin, K. Peters, H. G. von Schnering in *Proceedings of VIth European Conference on Solid-State Chemistry*, Zurich, **1997**.
[41] J.-C. Gabriel, K. Boubekeur, P. Batail, *Inorg. Chem.* **1993**, *32*, 2894.
[42] D. Fenske, personal communication.
[43] D. Fenske, J. Ohmer, *Angew. Chem.* **1987**, *99*, 155; *Angew. Chem. Int. Ed. Engl.* **1987**, *26*, 148.
[44] Z. N. Chen, T. Yoshimura, M. Abe, Y. Sasaki, S. Ishizaka, H. B. Kim, N. Kitamura, *Angew. Chem.* **2001**, *113*, 245; *Angew. Chem. Int. Ed. Engl.* **2001**, *40*, 239.

Received: April 17, 2001 [F3202]